

Single-Dose Pharmacokinetics and Tolerability of the Oral Epidermal Growth Factor Receptor Inhibitor Mobocertinib (TAK-788) in Healthy Volunteers: Low-Fat Meal Effect and Relative Bioavailability of 2 Capsule Products

Clinical Pharmacology
in Drug Development
2021, 10(9) 1028–1043
© 2021 Millennium Pharmaceuticals,
Inc., a wholly owned subsidiary of
Takeda Pharmaceutical Company
Limited. Clinical Pharmacology in
Drug Development published by
Wiley Periodicals LLC on behalf of
American College of Clinical
Pharmacology
DOI: 10.1002/cpdd.951

Steven Zhang, Shu Jin, Celina Griffin, Zhongling Feng, Jianchang Lin, Mike Baratta, Rachael Brake, Karthik Venkatakrisnan, and Neeraj Gupta

Abstract

Mobocertinib (TAK-788) is a tyrosine kinase inhibitor under investigation for treatment of non-small cell lung cancer with activating *EGFR* exon 20 insertions. This study examined the safety; tolerability; pharmacokinetics (PK), including food effects; and bioavailability of mobocertinib in healthy volunteers. In part 1, fasted volunteers were randomized to placebo or mobocertinib in single-ascending-dose cohorts (20-160 mg). In part 2, mobocertinib (120/160 mg) was administered on day 1 of periods 1 and 2 under fasted or low-fat meal conditions (2-period, 2-sequence crossover design). In part 3, fasted volunteers received mobocertinib 160 mg in 1 of 2 capsule products on day 1 of periods 1 and 2 with 7-day washout. Safety and PK parameters were assessed. Sixty-nine volunteers were enrolled (mean age, 29 years; 75% male). The most common adverse events (AEs; $\geq 10\%$ of volunteers) were gastrointestinal AEs (25%-50%) and headache (8%-31%). No serious AEs were reported. A low-fat meal did not affect the PK of mobocertinib or its active metabolites. The geometric mean terminal disposition phase half-life (20 hours) supported once-daily dosing. The 2 capsule products were bioequivalent. These data guided dosing and supported administration of mobocertinib without regard to low-fat meal intake in ongoing and planned clinical studies.

Keywords

EGFR exon 20, food effect, non-small cell lung cancer, safety, tyrosine kinase inhibitor

Non-small cell lung cancer (NSCLC) accounts for $\approx 84\%$ of lung cancer cases, with adenocarcinoma (50%) and squamous cell carcinoma (23%) being the most common histologic subtypes.¹ Epidermal growth

factor receptor (EGFR, also known as human epidermal growth factor receptor-1) is 1 of 4 members of the ErbB family of receptor tyrosine kinases that, when phosphorylated following endogenous ligand

Millennium Pharmaceuticals, Inc., Cambridge, Massachusetts, USA, a wholly owned subsidiary of Takeda Pharmaceutical Company Limited

This is an open access article under the terms of the Creative Commons Attribution-NonCommercial-NoDerivs License, which permits use and distribution in any medium, provided the original work is properly cited, the use is non-commercial and no modifications or adaptations are made.

Submitted for publication 22 October 2020; accepted 7 March 2021.

Corresponding Author:

Steven Zhang, PhD, Associate Scientific Director, Millennium Pharmaceuticals, Inc., 40 Landsdowne Street, Cambridge, MA 02139
(e-mail: Steven.Zhang@Takeda.com)

Karthik Venkatakrisnan and Neeraj Gupta are fellows of the American College of Clinical Pharmacology.

Karthik Venkatakrisnan was an employee of Millennium Pharmaceuticals, Inc., Cambridge, MA, USA, a wholly owned subsidiary of Takeda Pharmaceutical Company Limited, at the time the study was conducted. Current affiliation: EMD Serono, Inc., Billerica, Massachusetts.

binding, activate signal transduction pathways that regulate cellular proliferation and apoptosis.² In patients with NSCLC, in-frame deletions in *EGFR* exon 19 and a Leu858Arg (L858R) substitution in exon 21 together account for ≈90% of activating mutations, and patients with these mutations have a greater magnitude response to EGFR tyrosine kinase inhibitors (TKIs).²

Among the less common genetic drivers of NSCLC, approximately 4% to 9% of *EGFR*-mutated tumors harbor *EGFR* exon 20 insertion mutations,³⁻⁷ representing 1.7% to 3.4% of NSCLC cases.^{5,8} Like the more common mutations, these are overrepresented among never-smokers and Asian patients, suggesting they are driver mutations with the potential for durable responses following targeted therapy.^{4,9} However, exon 20 insertion mutations confer resistance to all approved EGFR TKIs (erlotinib, gefitinib, afatinib, and osimertinib), with their recommended phase 2 doses associated with only minimal benefit and poorer survival (median progression-free survival of ≈2 months) compared with TKI-sensitive *EGFR*-mutated NSCLC.^{3-5,10-12} Another receptor tyrosine kinase within the ErbB family, human EGFR-2 gene (*HER2*), is mutated in 2% to 4% of patients with NSCLC. The majority of these *HER2* mutations are also exon 20 insertions.¹³⁻¹⁵

Therapeutic options for patients with NSCLC whose tumors harbor *EGFR* exon 20 insertion mutations or *HER2*-activating mutations are limited. Mobocertinib (TAK-788; ARIAD Pharmaceuticals, Inc, a wholly owned subsidiary of Takeda Pharmaceutical Company Limited, Cambridge, Massachusetts), a novel, investigational, next-generation TKI, has potent preclinical inhibitory activity against activating *EGFR* and *HER2* mutations, including exon 20 insertions, and demonstrates stronger inhibition of these variants than wild-type (WT) *EGFR*.¹⁶ In an ongoing first-in-human phase 1/2 study of mobocertinib (NCT02716116), preliminary data indicated a median time to maximum plasma concentration (t_{max}) of 4 hours, and dose-proportional maximum plasma concentration (C_{max}) and area under the concentration-time curve (AUC) from time 0 to 24 hours. On repeat dosing at 160 mg once daily, accumulation ratio of mobocertinib AUC from time 0 to 24 hours on cycle 2 day 1 over cycle 1 day 1 was 1.03, which is smaller than the calculated accumulation ratio based on its terminal half-life and dose interval, suggesting autoinduction of mobocertinib apparent oral clearance via induction of cytochrome P450 (CYP) 3A at and above the 160-mg dose. Overall, metabolism appears to be the major route of clearance for mobocertinib. In vitro studies using recombinant human CYPs suggest that mobocertinib metabolism is primarily mediated by CYP3A4/5, as the percent

contribution of this enzyme was >90%. In preclinical studies, mobocertinib was eliminated almost completely through feces, and urinary and biliary excretion were insignificant. After metabolism of mobocertinib by CYP3A4/5, it was determined that there were 2 active metabolites, AP32960 and AP32914.¹⁷ Compared with the parent drug, AP32960 and AP32914 demonstrated comparable single-dose pharmacokinetics (PK) and similar pharmacodynamics preclinically, with similar in vitro potencies and specificities, ≈1% free fraction in plasma, similar inhibitory EGFR and HER2 cellular activity, and similar dose-dependent efficacy against EGFR- and HER2-driven NSCLC in vivo. The maximum tolerated dose for mobocertinib was identified as 160 mg once daily, and the scope and frequency of adverse events (AEs) was consistent within the broad class of other EGFR TKIs. Mobocertinib demonstrated clinical antitumor efficacy in patients with previously treated NSCLC with exon 20 insertion mutations, including those with brain metastases.¹⁸

The preferential inhibition of mutated *EGFR* over WT variants shown by mobocertinib preclinically suggests the potential to circumvent the dose-limiting toxicities (DLTs) that result from inhibition of WT *EGFR* in healthy tissues.^{19,20} On repeat dosing of mobocertinib in animal toxicology studies, 10 mg/kg was identified as the maximum tolerated dose based on predominantly dermal and gastrointestinal toxicities that were generally reversible; gonadal atrophy was reported as potentially irreversible, although the extent to which this was a direct drug effect as opposed to a response to stress and/or reduced food intake was unclear. In vitro assays showed no evidence of genotoxicity. The clinical pharmacology and preclinical safety data supported the current 3-part study of mobocertinib in healthy volunteers (NCT03482453). Consistent with the inclusion of healthy volunteers in previous clinical pharmacology studies of targeted agents,^{21,22} this study aimed to assess safety and tolerability of single-dose mobocertinib; to characterize the PK of mobocertinib and its active metabolites with and without a low-fat meal; and to assess the relative bioavailability of 2 capsule products of mobocertinib, in healthy volunteers.

Methods

Volunteers

Eligible volunteers were healthy adult nonsmokers (never or >20 years since last smoked) aged 18 to 55 years, with body weight ≥45 kg (women) or ≥55 kg (men), and body mass index of 18.0 to 30.0 kg/m². Key inclusion criteria were hepatic, renal, and bone marrow function within the normal ranges; normal baseline pulmonary function test (PFTs; ≥80% of predicted

normal for spirometry, lung volumes, and diffusion lung capacity) for enrollment in all 3 parts of the study; and normal screening chest computed tomography (CT) for enrollment in the dose-escalation (part 1) and food-effects (part 2) stages of the study. Key exclusion criteria included prior or ongoing pulmonary or cardiovascular disease; current or recent (≤ 3 months) gastrointestinal disease or signs of malabsorption; active infection or positive viral hepatitis or HIV serology; major surgery or blood transfusion within 4 weeks of mobocertinib administration; history of bleeding disorder; clinically significant abnormal laboratory assessments; and resting blood pressure $>140/90$ mm Hg or resting pulse <45 beats per minute. Patients who had received small-molecule drugs within 4 weeks or biologics within 16 weeks of mobocertinib administration; stomach acid-reducing agents within 2 weeks; or other prescription or over-the-counter medications within 1 week; or had consumed food or beverages containing grapefruit, orange, or pomegranate within 1 week of mobocertinib administration were also excluded.

The protocol and consent form were approved by the institutional review board (Midlands IRB, Overland Park, Kansas) before study initiation. All volunteers provided written informed consent. The study was performed in accordance with the requirements of the Declaration of Helsinki, the International Council for Harmonisation guidelines for Good Clinical Practice, and other applicable regulatory requirements.

Study Design

This study was conducted at a single site (PRA, Salt Lake City, Utah) in the United States and included 3 parts: a single-ascending-dose phase (part 1), a food-effect study (part 2), and a relative bioavailability study of 2 capsule products (part 3).

Part 1: Dose Escalation. Five cohorts of 8 fasted volunteers were randomly assigned (6:2) to receive a single oral dose of mobocertinib or placebo (Figure 1A). The first cohort received a single 20-mg dose, and each subsequent cohort received a single dose of mobocertinib 40, 80, 120, or 160 mg administered with 240 mL of water following an overnight fast of at least 10 hours. Volunteers were not allowed to eat for 4 hours after drug administration or drink additional water within 1 hour before or after drug administration. The starting dose of 20 mg was determined on the basis of clinical safety/tolerability data from the phase 1 study in patients with NSCLC and supported by preclinical safety data. Dose escalation proceeded on confirmation that there were no DLTs observed, and that all grade ≥ 2 treatment-related AEs had resolved to grade ≤ 1 within 5 days after administration in the previous dosing cohort. A DLT was defined as any grade ≥ 3 nonhematologic or hematologic toxicity or laboratory

abnormality that occurred ≤ 5 days following mobocertinib dosing and was considered at least possibly related to therapy. DLT assessment was repeated on days 8 and 15, if necessary, before proceeding to the next higher dose. A dose was considered tolerable if no more than 1 of 6 volunteers experienced a DLT within 5 days of dosing. Part 1 was conducted double-blind, although site staff and investigators were unblinded once volunteers left the study site.

Part 2: Effect of a Low-Fat Meal. Part 2 evaluated the effect of a low-fat meal on the PK of mobocertinib using an open-label 2-way crossover design (Figure 1B). Because it was unknown whether a low-fat meal would increase the systemic exposure of mobocertinib and potentially compromise the safety of healthy volunteers at the highest dose studied in part 1 (160 mg), the starting dose selected for a pilot study for part 2 was 120 mg. Based on evidence of tolerability at the 120-mg dose, the mobocertinib dose was then increased to 160 mg, the highest dose tolerated in part 1, under fasted conditions. All volunteers enrolled in part 2 were randomized (1:1) to receive a single oral dose of mobocertinib (120 mg, $n = 6$; 160 mg, $n = 10$) on day 1 (period 1), either under fasted conditions (overnight fast of at least 10 hours) or with a low-fat meal (≤ 350 calories and $\leq 15\%$ of calories from fat; meal eaten 30 minutes before drug administration). After a 7-day washout, mobocertinib was administered under the alternate treatment condition on day 8 (period 2). Under both conditions, mobocertinib was administered with 240 mL of water, no food was permitted for at least 4 hours after dosing, and no additional water was allowed for 1 hour before and after drug administration. Comparable to the low-fat meal described in the US Food and Drug Administration guidance for food-effect bioavailability studies (400–500 calories), the low-fat meal provided 336 calories, 46 (14% of total calories) from fat (5.1 g), 253 (75%) from carbohydrates (63.3 g), and 37 (11%) from protein (9.3 g). The meal comprised 2 slices of toasted white bread, 1 teaspoon of low-fat margarine, 1 tablespoon of jam, and 5 ounces of apple juice. Based on mobocertinib's high permeability and solubility, a low-fat meal was not expected to increase bioavailability of mobocertinib. The 7-day washout period between periods 1 and 2 could be adjusted to ensure that observed plasma trough concentration 168 hours after dosing in period 1 was $<5\%$ of the observed C_{\max} at the corresponding dose.

Part 3: Relative Bioavailability of 2 Capsule Products. Volunteers enrolled in part 3 were randomly assigned (1:1) to receive a single oral 160-mg dose of mobocertinib administered as capsule A (filled with mobocertinib manufactured in process A) or capsule B (filled with mobocertinib manufactured in process B) in an open-label 2-way crossover design with a 7-day washout



Figure 1. Design of this 3-part study of mobocertinib in healthy volunteers. (A) Part 1, a phase I, randomized, double-blind, placebo-controlled, single-rising-dose-escalation study. (B) Part 2, an open-label crossover evaluation of the effects of a low-fat meal on the PK of mobocertinib. (C) Part 3, an open-label crossover evaluation of bioavailability of mobocertinib capsule B relative to capsule A. D, day; PK, pharmacokinetics.

Table 1. Summary of Baseline Demographics (Safety Population)

Part 1 (Dose-Escalation Study)	Pooled Placebo (n = 10)	Mobocertinib					Overall (N = 40)
		20 mg (n = 6)	40 mg (n = 6)	80 mg (n = 6)	120 mg (n = 6)	160 mg (n = 6)	
Age, y, mean (SD)	34 (8)	28 (5)	29 (9)	25 (4)	27 (7)	31 (16)	29 (9)
Male, n (%)	7 (70)	6 (100)	5 (83)	4 (67)	3 (50)	5 (83)	30 (75)
Race, n (%)							
White	9 (90)	6 (100)	6 (100)	6 (100)	6 (100)	6 (100)	39 (98)
Black	1 (10)	0	0	0	0	0	1 (3)
BMI, kg/m ² , mean (SD)	25.6 (2.7)	26.7 (1.6)	23.9 (4.1)	21.8 (2.5)	23.9 (2.5)	25.3 (1.8)	24.6 (2.9)

Part 2 (Food Effect Study)	Mobocertinib 120 mg			Mobocertinib 160 mg		
	Low-Fat Meal →Fasted (n = 3)	Fasted→ Low-Fat Meal (n = 3)	Overall (N = 6)	Low-Fat Meal →Fasted (n = 5)	Fasted→ Low-Fat Meal (n = 5)	Overall (N = 10)
Age, y, mean (SD)	35 (9)	22 (2)	28 (9)	30 (12)	28 (11)	29 (11)
Male, n (%)	2 (67)	2 (67)	4 (67)	4 (80)	4 (80)	8 (80)
Race, n (%)						
White	3 (100)	3 (100)	6 (100)	5 (100)	4 (80)	9 (90)
Black	0	0	0	0	1 (20)	1 (10)
BMI, kg/m ² , mean (SD)	26.5 (2.3)	22.9 (2.5)	24.7 (2.9)	23.7 (3.5)	27.0 (2.7)	25.3 (3.5)

Part 3 (Relative Bioavailability Study)	Mobocertinib 160 mg		Overall (N = 13)
	Capsule B→Capsule A (n = 7)	Capsule A→Capsule B (n = 6)	
Age, y, mean (SD)	31 (11)	29 (12)	30 (11)
Male, n (%)	5 (71)	5 (83)	10 (77)
Race, n (%)			
White	7 (100)	5 (83)	12 (92)
Black	0	1 (17)	1 (8)
BMI, kg/m ² , mean (SD)	25.6 (1.4)	26.3 (3.0)	25.9 (2.2)

BMI, body mass index; SD, standard deviation.

period between doses (Figure 1C). Mobocertinib was administered with 240 mL of water after an overnight fast of at least 10 hours on days 1 and 8. No food was permitted for at least 4 hours after dosing; water was allowed except for 1 hour before and after drug administration. Mobocertinib synthesized by the different processes was chemically identical but differed in physical properties. The powder prepared in process B has larger particles, lower specific surface area, and higher bulk density than powder prepared using process A. The relative bioavailability of the 2 capsule products was assessed to enable PK bridging across patients taking the 2 different products in the mobocertinib clinical development program.

Safety Assessments

Safety evaluations included AEs, vital signs, chest CTs, electrocardiograms, laboratory assessments (hematol-

ogy, clinical chemistry, urinalysis), PFTs, and physical examinations. All AEs were recorded from the time of informed consent signing to 30 days after the final dose of mobocertinib, with follow-up phone calls on day 30 (part 1) or day 38 (parts 2 and 3). AEs were coded using Medical Dictionary for Regulatory Activities (version 21.0) terminology, and the severity of AEs was graded using National Cancer Institute Common Terminology Criteria for Adverse Events version 5.0. PFTs were performed 48 hours after dosing (part 1) or on day 3 of each period (parts 2 and 3), and/or early termination, if indicated on the basis of respiratory symptoms. Chest CT was performed if clinically indicated on day 3 of each period.

Pharmacokinetic Assessments

In the dose-escalation study (part 1), blood samples for PK analysis were collected before dosing and 0.5, 1, 2,

Table 2. Summary of AEs (Safety Population)

Part 1 (Dose-Escalation Study)	Pooled Placebo (n = 10)	Mobocertinib					Overall (N = 40)
		20 mg (n = 6)	40 mg (n = 6)	80 mg (n = 6)	120 mg (n = 6)	160 mg (n = 6)	
Any AE	2 (20)	2 (33)	3 (50)	4 (67)	3 (50)	5 (83)	19 (48)
Grade 1	2 (20)	2 (33)	2 (33)	3 (50)	1 (17)	4 (67)	14 (35)
Grade 2	0	0	1 (17)	1 (17)	2 (33)	1 (17)	5 (13)
Grade ≥3	0	0	0	0	0	0	0
Treatment-related AE	2 (20)	1 (17)	0	3 (50)	0	3 (50)	9 (23)
AE leading to discontinuation	0	0	0	0	0	0	0

Part 2 (Food-Effect Study)	Mobocertinib 120 mg		Mobocertinib 160 mg		Overall (N = 16)
	Low-Fat Meal (n = 6)	Fasted (n = 6)	Low-Fat Meal (n = 10)	Fasted (n = 10)	
Any AE	3 (50)	3 (50)	7 (70)	5 (50)	12 (75)
Grade 1	2 (33)	2 (33)	7 (70)	5 (50)	11 (69)
Grade 2	0	1 (17)	0	0	0
Grade ≥3	1 (17)	0	0	0	1 (6)
Treatment-related AE	2 (33)	3 (50)	4 (40)	5 (50)	8 (50)
Grade ≥3	0	0	0	0	0
AE leading to discontinuation	0	0	0	0	0

Part 3 (Relative Bioavailability Study)	Mobocertinib 160 mg		Overall (N = 13)
	Capsule B (n = 13)	Capsule A (n = 12)	
Volunteers with AEs, n (%)	4 (31)	4 (33)	6 (46)
Grade 1	4 (31)	3 (25)	5 (39)
Grade 2	0	1 (8)	1 (8)
Grade ≥3	0	0	0
Treatment-related AE	1 (8)	2 (17)	2 (15)
AE leading to discontinuation	1 (8)	0	1 (8)

AE, adverse event.

Data are n (%).

4, 6, 8, 12, 24, 36, 48, 72, 96, and 168 hours after dosing and urine samples were collected before dosing and 12, 24, 36, and 48 hours after dosing. In the food-effect study (part 2), blood samples were collected before dosing and 0.5, 1, 2, 4, 6, 8, 12, 24, 36, 48, 72, 96, and 168 hours after dosing. In the relative bioavailability study (part 3), blood samples were collected before dosing and 0.5, 1, 2, 4, 6, 8, 12, 24, 36, 48, and 72 hours after dosing.

Blood samples were collected in chilled tubes containing potassium ethylenediaminetetraacetic acid and centrifuged within 60 minutes of collection. Following centrifugation, aliquots of harvested plasma were added to separate vials and stored at -70°C . Plasma concentrations of mobocertinib, AP32914, and AP32960 in human plasma were determined by a validated sensitive and specific liquid chromatography–tandem mass spectrometry (LC-MS/MS)-based method. Following

thawing, a $50\text{-}\mu\text{L}$ plasma aliquot was added to a 96-well plate followed by $200\ \mu\text{L}$ of internal standard solution (0.500, 0.500, and 5.00 ng/mL of [^2H] mobocertinib, [^2H] AP32960, and [^2H] AP32914 in acetonitrile, respectively) while on wet ice. Plasma proteins were precipitated by the addition of $200\ \mu\text{L}$ of acetonitrile. The plate was covered, vortexed, and centrifuged before removal of a $100\text{-}\mu\text{L}$ aliquot for analysis using an API-5500 mass spectrometer (SCIEX, Framingham, Massachusetts) equipped with dual Agilent 1312B pumps (Agilent Technologies, Santa Clara, California) and a Thermo PAL autosampler (Thermo Fisher Scientific, Waltham, Massachusetts). A reverse-phase gradient method running at a flow rate of $0.45\ \text{mL}/\text{min}$ on an XTERRA C18, $2.1 \times 50\ \text{mm}$, $3.5\ \mu\text{m}$ column (Waters Corporation, Milford, Massachusetts) provided AP32914, AP32960, and mobocertinib retention times of 1.88,

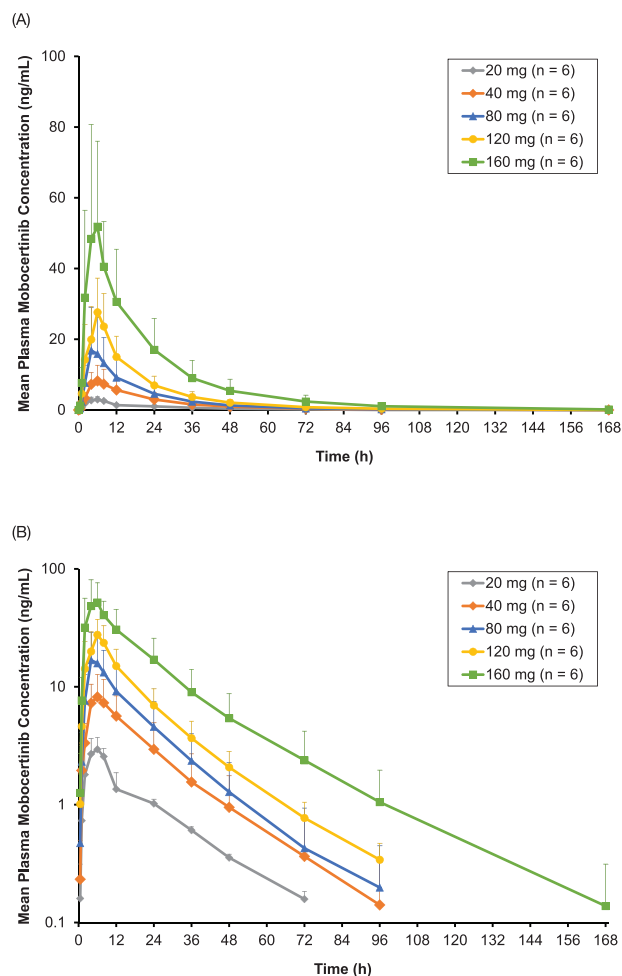


Figure 2. Mean (\pm SD) plasma mobocertinib concentrations following single oral doses of 20 mg to 160 mg mobocertinib during dose-escalation (part I) plotted on (A) linear and (B) log-linear scales. SD, standard deviation.

2.39, and 2.49 (\pm 0.4) minutes. The mobile phases used were (5:95:0.5) methanol, 2.5 mM ammonium acetate in water, and NH_4OH in water (A); and (20:80) acetonitrile, methanol (B). Mobocertinib, AP32914, AP32960, and the respective internal standards were ionized under a positive ion spray mode and detected through multiple reaction monitoring of mass transition pairs at m/z (mobocertinib/internal standard) 586.0 \rightarrow 72.1 and 591.0 \rightarrow 72.1, (AP32914/internal standard) 572.2 \rightarrow 72.1 and 577.2 \rightarrow 72.2, and (AP32960/internal standard) 572.2 \rightarrow 515.2 and 577.2 \rightarrow 520.2, respectively. Calibration curves for each analyte were established using standards, and the peak area ratios of the analyte against the isotopically labeled internal standard were used to quantify samples. Linearity was achieved in the mobocertinib concentration range of 0.100 to 100 ng/mL with quality control samples ranging from 0.300 to 80.0 ng/mL. Incurred sample reanalysis of plasma samples met acceptance criteria.

Urine samples were fortified (1:1, v:v) with isopropyl alcohol (IPA) because of nonspecific binding of mobocertinib, AP32914, and AP32960 to plastic. Following centrifugation, aliquots of harvested IPA-fortified urine were added to separate vials and stored at -70°C . Concentrations of mobocertinib, AP32914, and AP32960 in IPA-fortified human urine were determined by a validated sensitive and specific LC-MS/MS-based method. Following thawing, a 25- μL fortified urine aliquot was added to a 96-well plate followed by 200 μL of internal standard solution (5.00, 0.500, and 5.00 ng/mL of [^2H] mobocertinib, [^2H] AP32960, and [^2H] AP32914 in acetonitrile, respectively) while on wet ice. Urine proteins were precipitated by the addition of 200 μL of acetonitrile. The plate was covered, vortexed, and centrifuged before removal of a 50- μL aliquot, which was diluted with 200 μL of (95:5:0.5, v:v:v) 2.5 mM ammonium acetate in water, methanol, and NH_4OH water. The plate was covered and vortexed before injection. The LC-MS/MS setup was a Sciex API-5500 mass spectrometer equipped with dual Agilent 1312B pumps and a Thermo PAL autosampler. A reverse-phase gradient method running at a flow rate of 0.450 mL/min on a Waters XTERRA C18, 2.1 \times 50 mm, 3.5 μm column provided AP32914, AP32960, and mobocertinib retention times of 1.00, 1.25, and 1.60 (\pm 0.2) minutes. The mobile phases used were (95:5:0.5, v:v:v) 2.5 mM ammonium acetate in water, methanol, and NH_4OH water (1) and (20:80, v:v) acetonitrile:methanol (2). Mobocertinib, AP32914, AP32960, and the respective internal standards were ionized under a positive ion spray mode and detected through multiple reaction monitoring of mass transition pairs at m/z (mobocertinib/internal standard) 586.4 \rightarrow 72.1 and 591.4 \rightarrow 72.1, (AP32914/internal standard) 572.4 \rightarrow 72.1 and 577.4 \rightarrow 72.2, and (AP32960/internal standard) 572.4 \rightarrow 515.3 and 577.4 \rightarrow 520.3, respectively. Calibration curves for mobocertinib, AP32914, and AP32960 were established using standards, and the peak area ratios of the analyte against the isotopically labeled internal standard were used to quantify samples. Linearity was achieved in the mobocertinib concentration range of 1.00 to 1000 ng/mL with quality control samples ranging from 3.00 to 800 ng/mL. Incurred sample reanalysis of urine samples met acceptance criteria.

In part I, plasma PK parameters were estimated for mobocertinib, AP32960, and AP32914; these included C_{max} , t_{max} , AUC from time 0 to time of the last quantifiable concentration (AUC_{last}); AUC from time 0 to infinity, calculated using the observed value of the last quantifiable concentration (AUC_{∞}); combined molar C_{max} and AUC_{∞} of mobocertinib, AP32960, and AP32914; the apparent clearance after extravascular administration (CL/F); and the terminal disposition

phase half-life ($t_{1/2z}$). For the preliminary assessment of urinary excretion of mobocertinib after oral administration, the following parameters were estimated: amount of drug excreted in urine from time 0 to 48 hours after dosing and fraction of administered dose of drug excreted in urine from time 0 to the last collection time. In parts 2 and 3, C_{\max} , t_{\max} , and AUC_{∞} were estimated for mobocertinib, and the combined molar C_{\max} and AUC_{∞} were estimated including mobocertinib, AP32960, and AP32914.

Pharmacokinetic and Statistical Analyses

In part 1, the sample size (approximately $n = 56$) was determined based on clinical rather than statistical considerations, consistent with phase 1 dose-finding studies. For part 2, a sample size of 14 volunteers was anticipated to result in a 90% confidence interval (CI) of 84% to 119% for the AUC ratio based on within-individual AUC variability of 27% in patients with NSCLC and a mobocertinib AUC ratio of 1 in the fed-vs-fasted comparison. Assuming 2 potential dropouts, the total planned sample size was therefore 16 volunteers. For part 3, a sample size of 10 healthy volunteers was anticipated to result in a 90%CI of 87% to 115% for the C_{\max} ratio using a within-individual C_{\max} variability of 17% estimated in healthy volunteers. Assuming 2 potential dropouts, the planned sample size was 12 volunteers.

Safety was analyzed in the safety populations for each study part, which included all volunteers who received at least 1 dose of mobocertinib. PK parameters were analyzed in the PK population, which included all volunteers in the safety populations with sufficient data to complete PK analyses.

Plasma PK parameters for mobocertinib and its metabolites AP32960 and AP32914 were estimated by noncompartmental methods, applying the linear trapezoidal methods, using Phoenix WinNonlin, version 8.1 (Certara, Princeton, New Jersey). Urine PK parameters were estimated using SAS version 9.4 (SAS Institute, Cary, North Carolina). Plasma or urine concentrations below the limit of quantification (BLQ) were treated as 0 in the summarization of concentration values. When deriving plasma PK parameters, BLQ results occurring before t_{\max} were treated as 0, whereas those occurring after t_{\max} were treated as missing.

In parts 2 and 3, the effects of a low-fat meal and the relative bioavailability of the 2 capsule products, respectively, were assessed using an analysis of variance on log-transformed PK parameters including C_{\max} and AUC_{∞} of mobocertinib and combined molar C_{\max} and AUC_{∞} of mobocertinib, AP32960, and AP32914 by dose level. The ratios of the geometric means of C_{\max} and AUC_{∞} , as well as the associated 2-sided 90% CIs, were calculated on the basis of the within-volunteer

variance, calculated via a mixed-effects analysis of variance fitting terms for either meal condition (fed vs fasted) in part 2 or treatment (capsule B vs capsule A) in part 3, with sequence and period as fixed effects. Volunteer within sequence was treated as a random effect in the model. Point estimates (least squares [LS] means) and adjusted 90% CIs for the differences of LS means between conditions were calculated and then exponentially back-transformed to provide point and 90%CI estimates for the ratios of PK parameters. Statistical tests were conducted using SAS version 9.4.

The dose proportionality of the PK of mobocertinib and its active metabolites was assessed based on pooled exposure data from all 3 parts of the study by fitting the observed data to the following power model using linear regression:

$$\ln(Y) = a + b \cdot \ln(\text{dose}) + \varepsilon$$

where Y was the AUC parameter (either mobocertinib AUC_{∞} or combined molar AUC_{∞} of mobocertinib, AP32960, and AP32914); a and b were the estimated intercept and slope parameters, respectively; dose was the mobocertinib dose administered in milligrams; and ε was a normally distributed error term. The analysis was performed using SigmaPlot version 12.0 (Systat Software, San Jose, California). A value of b equal to 1.0 implied dose proportionality. If 1.0 was contained within the 95%CI for b , the data were considered consistent with dose proportionality. Exposure data included in the dose-proportionality analysis consisted of those following oral administration of mobocertinib 40 mg ($n = 6$), 80 mg ($n = 6$), 120 mg ($n = 6$), and 160 mg ($n = 6$) capsule B under fasted conditions in part 1; mobocertinib 120 mg ($n = 6$) and 160 mg ($n = 10$) capsule A under fasted conditions and with a low-fat meal in part 2; and mobocertinib 160 mg ($n = 12$) capsule A and capsule B under fasted conditions in part 3. In the crossover studies (parts 2 and 3), exposure data (AUC_{∞} and combined molar AUC_{∞}) from individual volunteers were counted from both sequences for the dose-proportionality analysis. The combined molar AUC_{∞} from 6 volunteers ($n = 4$ at 40-mg dose, $n = 1$ at 80-mg dose, and $n = 1$ at 160-mg dose) was not included in the dose-proportionality analysis because AUC_{∞} for AP32914 could not be reliably estimated.

Baseline characteristics, safety, and tolerability were summarized using descriptive statistics. In part 1, data from placebo patients were pooled. PK parameters were summarized using descriptive statistics and presented by dose level in part 1, by low-fat meal vs fasted conditions in part 2, and by capsule B (test) vs capsule A (reference) in part 3.

Table 3. Summary of Plasma Mobocertinib PK Parameters After Single Oral Dosing in the Dose-Escalation Study (Part 1)

PK Parameter	Mobocertinib				
	20 mg (n = 6)	40 mg (n = 6)	80 mg (n = 6)	120 mg (n = 6)	160 mg (n = 6)
t_{\max} , h					
Median (range)	6.0 (2.0-8.1)	5.0 (4.0-6.0)	4.0 (4.0-8.0)	6.0 (2.0-6.0)	6.0 (4.0-6.0)
C_{\max} , ng/mL					
Mean (SD)	3.3 (0.9)	8.6 (4.2)	17.6 (11.6)	27.6 (9.7)	56.2 (27.7)
Geometric mean (% CV)	3.2 (28.2)	7.9 (49.0)	14.7 (66.1)	25.8 (35.0)	52.2 (49.3)
AUC_{last} , ng • h/mL					
Mean (SD)	60 (7.1)	180 (112.1)	301 (197.3)	485 (184.4)	1103 (596.1)
Geometric mean (% CV)	59 (11.8)	155 (62.2)	250 (65.5)	448 (38.0)	1008 (54.0)
AUC_{∞} , ng • h/mL					
Mean (SD)	64 (7.1)	186 (115.6)	308 (203.4)	494 (187.2)	1113 (599.1)
Geometric mean (% CV)	64 (11.1)	160 (62.1)	257 (66.0)	456 (37.9)	1017 (53.8)
CL/F, L/h					
Mean (SD)	316 (37.5)	283 (140.1)	378 (272.2)	292 (166.2)	168 (55.7)
Geometric mean (% CV)	314 (11.9)	249 (49.5)	312 (72.0)	263 (56.9)	157 (33.2)
$t_{1/2z}$, h					
Mean (SD)	18.1 (1.5)	16.0 (4.6)	14.8 (4.3)	18.3 (1.3)	20.5 (5.5)
Geometric mean (% CV)	18.1 (8.2)	16.0 (27.9)	14.3 (29.2)	18.3 (7.0)	19.9 (26.7)

AUC_{last} indicates area under the plasma concentration-time curve from time 0 to time of the last quantifiable concentration; AUC_{∞} , area under the plasma concentration-time curve from time 0 to infinity, calculated using the observed value of the last quantifiable concentration; CL/F, apparent clearance after extravascular administration; C_{\max} , maximum observed plasma concentration; CV, coefficient of variation; PK, pharmacokinetics; SD, standard deviation; $t_{1/2z}$, terminal disposition phase half-life; t_{\max} , time of first occurrence of C_{\max} .

Results

Volunteers

All enrolled volunteers were randomized and included in the safety populations (part 1: n = 40, including 10 volunteers randomized to placebo; part 2: n = 16; part 3: n = 13). All 30 volunteers who received mobocertinib in part 1, 16 volunteers in part 2, and 12 in part 3 (1 excluded due to vomiting) were included in the respective PK analysis populations. Demographic characteristics are shown in Table 1. The mean age was 29.3 years in part 1, 28.3 (120-mg dose group) and 28.8 years (160-mg dose group) in part 2, and 30.1 years in part 3. The majority of volunteers were men (75.0%, 75.0%, and 76.9% parts 1, 2, and 3, respectively) and white (97.5%, 93.8%, and 92.3%, respectively). Mean body mass index was 24.6 kg/m² in part 1, 24.7 kg/m² (120 mg) and 25.3 kg/m² (160 mg) in part 2, and 25.9 kg/m² in part 3.

Safety and Tolerability of Mobocertinib

AEs are summarized in Table 2. In all, 48% of volunteers in part 1, 75% in part 2, and 46% in part 3 experienced AEs. The most common AEs experienced by ≥10% of volunteers in any part of the study were gastrointestinal (overall, 25%-50%; nausea, 12.5%-31.3%; flatulence, 12.5%; soft feces, 12.5%; diarrhea, 10.0%; upper abdominal pain, 5.0%-18.8%) and headache (7.5%-31.3%). One volunteer who received

160-mg mobocertinib in part 1 had a grade 2 AE of increased lipase that was determined to be drug related and resolved without intervention. In part 2, 1 volunteer who received 120-mg mobocertinib had a grade 3 AE of increased lipase and a grade 2 AE of increased amylase, both due to gluten intolerance and therefore deemed not to be drug related; both events resolved without treatment. All other AEs were grade 1 or 2. All AEs recovered or resolved. One AE (grade 1 vomiting in 1 volunteer in part 3) led to treatment discontinuation. No serious AEs were reported. There were no clinically significant changes in serum hematology, urinalysis, vital signs, physical examination, or electrocardiogram results. Marked decreases in serum creatine kinase were observed (ranging from -26.8 U/L in the 20-mg dose group to -69.0 U/L in the 160-mg group, versus -46.6 U/L in the pooled placebo group) but a dose-dependent effect was not apparent. PFTs remained normal throughout.

Plasma PK of Mobocertinib After Single Oral Dosing

After single oral doses, mean plasma concentrations of mobocertinib increased with increasing dose (Figures 2A and 2B). Mobocertinib was quantifiable in plasma for up to 72 hours in the 20-mg cohort; 96 hours in the 40-, 80-, and 120-mg cohorts; and 168 hours in the 160-mg cohort. After reaching peak concentrations within 4.0 to 6.0 hours across the dose range, concentration

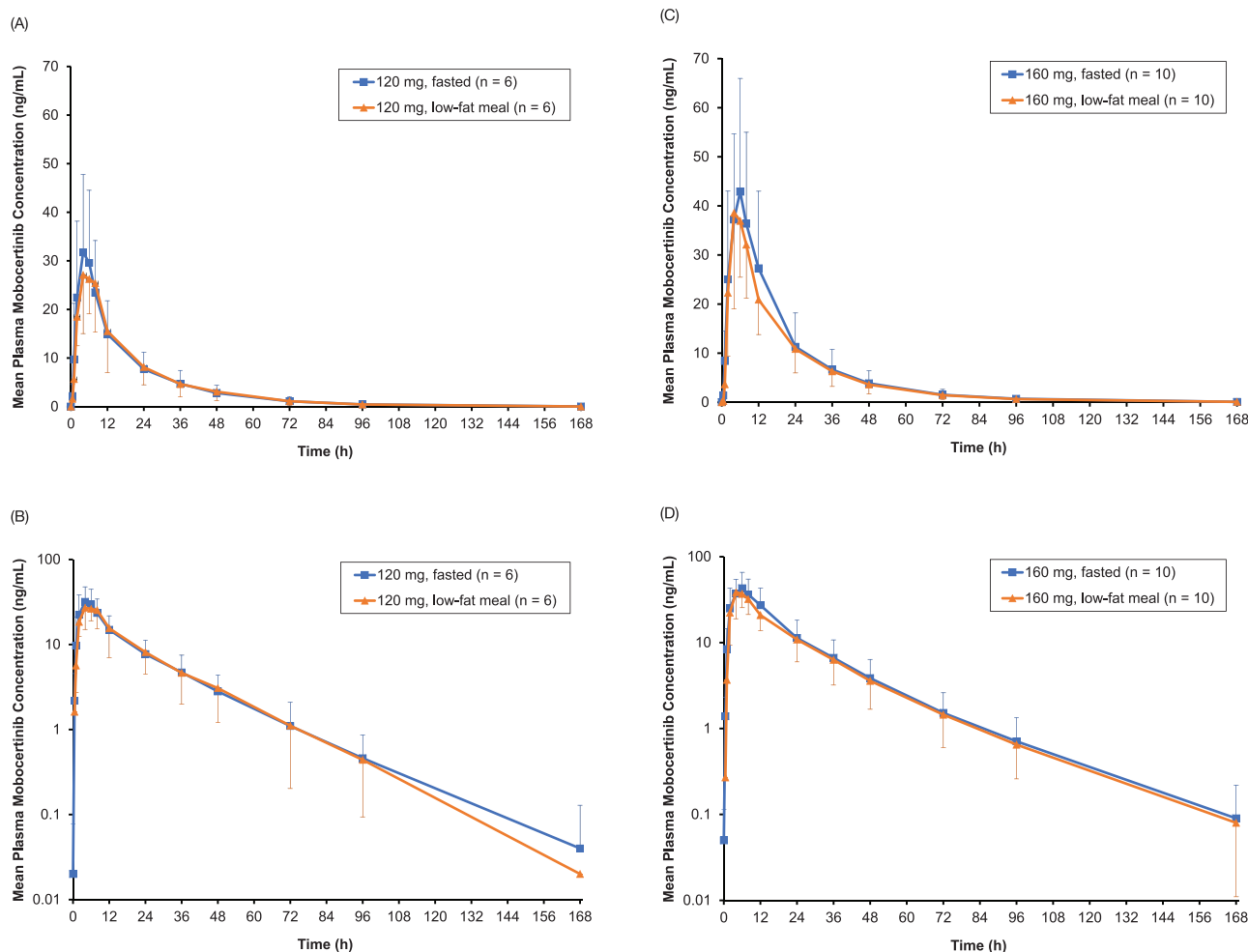


Figure 3. Mean (\pm SD) plasma mobocertinib concentration-time profiles following a single oral dose of mobocertinib (A-B) 120 mg or (C-D) 160 mg administered after a low-fat meal or under fasted conditions (part 2) plotted on (A, C) linear and (B, D) log-linear scales. SD, standard deviation.

decreased in a multiexponential manner with a similar elimination rate across the dose range. A summary of PK parameters is provided in Table 3. There were no dose-related trends in $t_{1/2z}$ or CL/F .

Plasma PK of Mobocertinib Active Metabolites After Single Oral Dosing

Mean plasma concentrations of the active metabolites AP32960 and AP32914 increased with increasing mobocertinib dose across the full dose range for AP32960 (Figures S1A and S1B) and over the 40-mg to 160-mg dose range for AP32914 (Figures S2A and S2B). At every dose level, plasma concentrations of AP32960 were quantifiable for longer than those of AP32914 (20 mg: 72 hours versus BLQ, respectively; 40 mg and 80 mg: 96 vs 48 hours; 120 mg: 168 vs 48 hours; 160 mg: 168 vs 96 hours). Median t_{max} ranged from 4.0 to 6.0 hours for both

metabolites, similar to that of the parent drug. After reaching peak concentration, AP32960 concentration decreased in a multiexponential manner, whereas AP32914 concentrations decreased in a biexponential manner. The elimination rates were generally similar across the dose range evaluated for both metabolites.

A summary of PK parameters for both metabolites is provided in Table S1. Compared with AP32914, AP32960 demonstrated considerably higher C_{max} , AUC_{last} and AUC_{∞} , and longer $t_{1/2z}$. A summary of combined molar PK parameters for mobocertinib, AP32960, and AP32914 is in Table S2. The mean AP32960-to-mobocertinib molar AUC_{∞} ratios (range, 0.51-0.66) were considerably higher than those for AP32914 (0.07-0.09) from 40 mg to 160 mg (20-mg values were not derivable). There were no dose-related trends when comparing molar ratios for the 2 metabolites.

Table 4. Summary of Plasma PK Parameters of Mobocertinib and Assessment of the Effect of a Low-Fat Meal on Mobocertinib PK Exposure

Mobocertinib Dose Parameter	Fasted (Reference)	Low-Fat Meal (Test)	Geometric LS Mean Ratio (90%CI) (Test vs Reference)
120 mg	n = 6	n = 6	
t_{max} , h			
Median (range)	4.0 (2.0-6.0)	6.0 (4.0-8.0)	
C_{max} , ng/mL			
Mean (SD)	35.5 (16.7)	29.5 (11.4)	
Geometric mean (% CV)	31.2 (47.0)	27.5 (38.7)	0.88 (0.71-1.09)
AUC_{∞} , ng • h/mL			
Mean (SD)	587 (301.8)	578 (272.1)	
Geometric mean (% CV)	526 (51.4)	534 (47.1)	1.02 (0.90-1.15)
Combined molar ^a C_{max} , nM			
Mean (SD)	96.3 (40.0)	80.7 (25.1)	
Geometric mean (% CV)	88.0 (41.1)	77.3 (31.0)	0.88 (0.72-1.07)
Combined molar ^a AUC_{∞} , nM • h			
Mean (SD)	1643 (695.2)	1619 (615.0)	
Geometric mean (% CV)	1525 (42.3)	1535 (38.0)	1.01 (0.90-1.12)
160 mg	n = 10	n = 10	
t_{max} , h			
Median (range)	6.0 (2.0-12.0)	6.0 (2.0-8.0)	
C_{max} , ng/mL			
Mean (SD)	45.8 (21.9)	43.0 (17.2)	
Geometric mean (% CV)	41.0 (47.9)	39.5 (40.0)	0.96 (0.84-1.11)
AUC_{∞} , ng • h/mL			
Mean (SD)	862 (462.1)	768 (294.6)	
Geometric mean (% CV)	743 (53.6)	706 (38.4)	0.95 (0.87-1.03)
Combined molar ^a C_{max} , nM			
Mean (SD)	128 (52.3)	120 (39.5)	
Geometric mean (% CV)	119 (40.8)	113 (33.1)	0.95 (0.84-1.08)
Combined molar ^a AUC_{∞} , nM • h			
Mean (SD)	2584 (1162.3) ^b	2243 (733.3)	
Geometric mean (% CV)	2323 ^b (45.0)	2113 (32.7)	0.94 (0.87-1.03) ^b

AUC_{∞} , area under the concentration-time curve from time 0 to infinity, calculated using the observed value of the last quantifiable concentration; CI, confidence interval; C_{max} , maximum observed plasma concentration; CV, coefficient of variation; LS, least squares; PK, pharmacokinetics; SD, standard deviation; t_{max} , time of first occurrence of maximum observed plasma concentration.

A linear mixed-effect model on the natural log-transformed parameters was performed with regimen, sequence, and period as a fixed effect and volunteer nested within sequence as a random effect. The LS means and difference of LS means for the log-transformed parameters were exponentiated to obtain the point estimates and 90% CIs of the geometric LS mean ratio on the original scale.

^a Combined molar concentration and AUC_{∞} of mobocertinib, AP32960, and AP32914.

^b n = 9.

Urine PK of Mobocertinib After Single Oral Dosing

Within 48 hours, 0.63% to 1.16% of the administered mobocertinib dose was excreted unchanged in urine across all dose groups (Table S3), suggesting that mobocertinib is minimally eliminated via renal excretion.

Plasma PK of Mobocertinib After a Low-Fat Meal

After administration of mobocertinib 120 and 160 mg under low-fat meal and fasted conditions, mean plasma concentrations were quantifiable up to 168 hours in both dose cohorts (Figures 3A–3D). Concentration-time profiles in both dose groups with or without a

low-fat meal showed a similar rate of mobocertinib oral absorption and concentration decreasing gradually in a multiexponential manner, with a similar elimination rate. Plasma PK parameters were similar when mobocertinib was administered with a low-fat meal or under fasting conditions (Table 4). At the 120-mg dose, median t_{max} was 6.0 hours with a low-fat meal and 4.0 hours when fasted, compared with a median t_{max} of 6.0 hours under fed and fasted conditions following the 160-mg dose. Plasma geometric mean C_{max} and AUC_{∞} of mobocertinib and geometric mean combined molar C_{max} , and AUC_{∞} of mobocertinib, AP32960, and

Table 5. Relative Bioavailability Assessment of Mobocertinib (160 mg) After Oral Administration of Capsule B Compared With Capsule A Under Fasted Conditions

Parameter	Capsule A (Reference)	Capsule B (Test)	LS Geometric Mean Ratio (90%CI) (Test vs Reference)
	n = 12	n = 12	
t_{max} , h			
Median (range)	6.0 (2.0-8.0)	5.0 (2.0-8.0)	
C_{max} , ng/mL			
Mean (SD)	46.8 (14.7)	43.4 (11.9)	
Geometric mean (% CV)	44.8 (31.5)	41.7 (27.5)	0.93 (0.85-1.03)
AUC_{∞} , ng • h/mL			
Mean (SD)	761 (193.1)	754 (262.8)	
Geometric mean (% CV)	739 (25.4)	710 (34.9)	0.96 (0.89-1.04)
Combined molar ^a C_{max} , nM			
Mean (SD)	134.3 (37.1)	124.5 (30.9)	
Geometric mean (% CV)	130 (27.6)	121 (24.8)	0.93 (0.87-1.00)
Combined molar ^a AUC_{∞} (nM • h)			
Mean (SD)	2247 (516.8)	2177 (668.1)	
Geometric mean (% CV)	2194 (23.0)	2079 (30.7)	0.95 (0.89-1.01)

AUC_{∞} , area under the concentration-time curve from time 0 to infinity, calculated using the observed value of the last quantifiable concentration; CI, confidence interval; C_{max} , maximum observed plasma concentration; CV, coefficient of variation; PK, pharmacokinetics; SD, standard deviation; t_{max} , time to maximum observed plasma concentration.

A linear mixed-effect model on the natural log-transformed parameters was performed with regimen, sequence, and period as a fixed effect and volunteer nested within sequence as a random effect. The least squares (LS) means and difference of LS means for the log-transformed parameters were exponentiated to obtain the point estimates and 90% CIs of the geometric LS mean ratio on the original scale.

^a Combined molar concentration and AUC_{∞} of mobocertinib, AP32960, and AP32914.

AP32914 were similar under low-fat meal and fasted conditions after 120 mg and 160 mg mobocertinib (Table 4). With the 160-mg dose, the LS geometric mean ratio under low-fat meal vs fasted conditions was 0.96 (90%CI, 0.84-1.1) for C_{max} and 0.95 (90%CI, 0.87-1.03) for AUC_{∞} . The 90% CIs for the LS geometric mean ratios between low-fat meal and fasted states for the combined molar C_{max} and AUC_{∞} of mobocertinib, AP32960, and AP32914 also fell within the 80% to 125% equivalence limits after the 160-mg dose. Data were similar at 120 mg, although the lower bound of the 90%CI for C_{max} and combined molar C_{max} ratios dropped below the 80% lower bound of the acceptance 90%CI due to the small sample size of 6.

Relative Bioavailability of Mobocertinib Administered as Different Capsule Products

Mean plasma concentrations of mobocertinib were measured up to 72 hours after a single 160-mg dose administered as capsule A or B, with similar concentration-time profiles between products (Figures 4A and 4B). Mobocertinib was absorbed at a moderate rate with median t_{max} between 5 and 6 hours. After peaking, plasma concentrations decreased gradually in a multiexponential manner with a similar elimination rate between products. Mean plasma C_{max} and

AUC_{∞} of mobocertinib and combined molar C_{max} and AUC_{∞} of mobocertinib, AP32960, and AP32914 were similar regardless of capsule product (Table 5). For mobocertinib alone, the LS geometric mean ratios for C_{max} and AUC_{∞} were 0.93 (90%CI, 0.85-1.03) and 0.96 (90%CI, 0.89-1.04), respectively. All 90% CIs were contained within the 80% to 125% equivalence limits, demonstrating bioequivalence between the 2 mobocertinib capsule products.

Mobocertinib Dose Proportionality

Approximate dose proportionality was observed over the 40- to 160-mg dose range, with calculated slopes (95% CIs) of the regression line using log-transformed data of 1.20 (0.93-1.46) and 1.14 (0.84-1.44) for the relationship between mobocertinib AUC_{∞} and dose, and between combined molar AUC_{∞} (for mobocertinib, AP32960, and AP32914) and dose, respectively (Figures 5A and 5B).

Discussion

This study was the first to evaluate the safety, tolerability, and PK properties of mobocertinib in healthy volunteers. The dose-escalation part of the study was conducted in healthy volunteers, in alignment with phase 1 single-dose clinical pharmacology studies

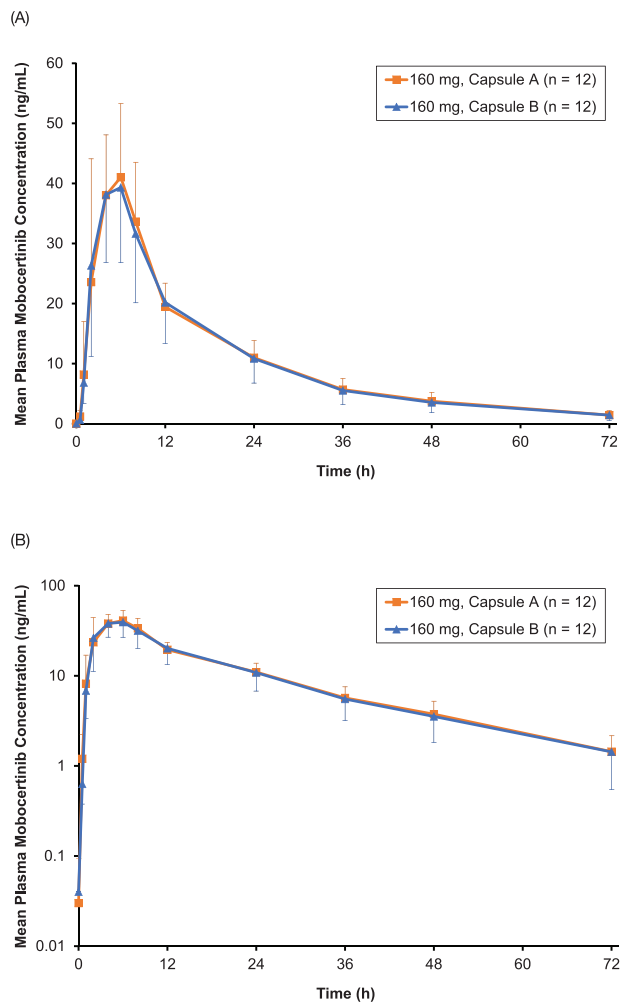


Figure 4. Mean (\pm SD) plasma mobocertinib concentration-time profiles following a single oral dose of mobocertinib 160 mg in capsule A or capsule B products, administered under fasted conditions, plotted on (A) linear and (B) log-linear scales. SD, standard deviation.

of other oral TKIs.^{23–25} The low-fat meal and relative bioavailability parts of the study were designed in accordance with appropriate US Food and Drug Administration guidance.

Single doses of mobocertinib up to 160 mg were tolerated in healthy adult volunteers. There was 1 grade 3 AE (increased lipase [without symptoms] that was unrelated to mobocertinib and required no treatment), and a single volunteer discontinued treatment due to grade 1 vomiting. There were no clinically relevant pulmonary, renal, hepatic, or cardiac abnormalities or serious AEs. The preponderance of gastrointestinal AEs is consistent with the AE profile for approved EGFR TKIs, which commonly cause diarrhea and are associated with AE-related treatment discontinuation in <10% of patients.^{26,27}

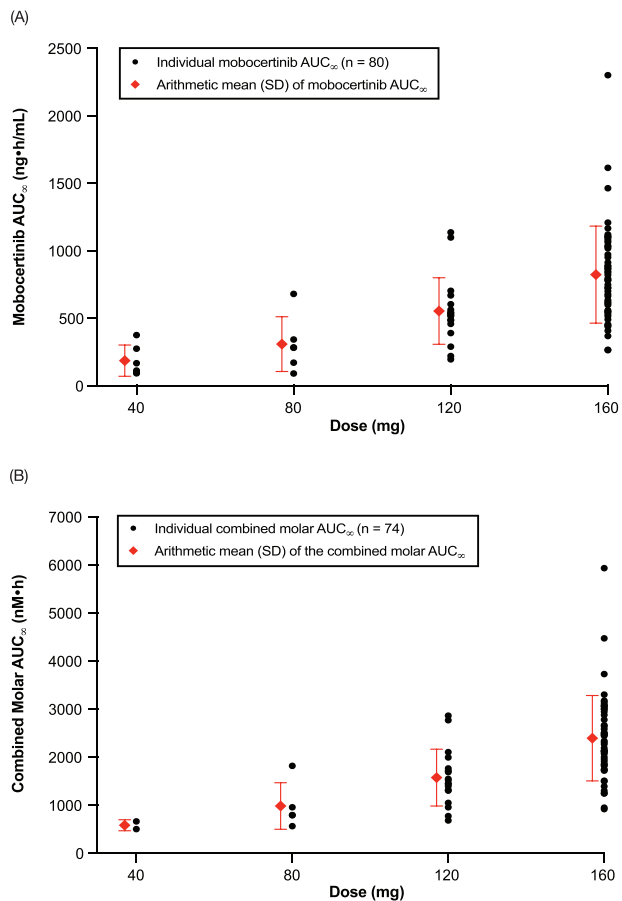


Figure 5. Dose proportionality of (A) plasma mobocertinib AUC_{∞} and (B) combined molar AUC_{∞} of mobocertinib, AP32960, and AP32914 vs mobocertinib dose following single oral dose administration of mobocertinib. AUC_{∞} indicates area under the concentration-time curve from time 0 to infinity. Mean and SD bars were moved to the left by 2 units during plotting for visualization. SD, standard deviation.

After single oral doses, mobocertinib was systemically absorbed and reached peak concentrations after 4 to 6 hours. The reported geometric mean $t_{1/2z}$ of 20 hours justifies the once-daily dosing regimen used in patients with cancer. Systemic exposure was approximately dose-proportional over the 40- to 160-mg dose range, and supports mobocertinib dose reduction as needed to manage AEs. The data reported in this study are consistent with preliminary mobocertinib PK data from a phase 1/2 study in patients with NSCLC (unpublished data), further supporting our conclusions. Both active metabolites of mobocertinib identified in *in vitro* studies were observed in human plasma samples, with t_{max} values in the same range as the parent drug, and dose-independent metabolite-to-parent ratios that did not reach saturation at doses \leq 160 mg. Urinary excretion of unchanged mobocertinib was minimal (<1.2% of the total dose) and was similar across the dose range,

suggesting that patients with mild or moderate renal impairment are unlikely to require dose modification.

Our development strategy involved conducting a low-fat meal study before a high-fat meal study to provide guidance on dosing in phase 2 and 3 trials. Low-fat meal studies have been conducted during development of many oral TKIs used for cancer treatment, including palbociclib, pazopanib, lapatinib, and ceritinib.^{21,28–32} While low-fat meal studies can be especially valuable for Biopharmaceutics Classification System Class II (low solubility, high permeability) drugs, which are likely to show positive food effects due to increased solubility in the fed state,³³ mobocertinib is a highly soluble Biopharmaceutics Classification System Class I compound, and the risk of food effects was expected to be low. If an effect was shown in a high-fat meal study, a low-fat meal study would still be necessary to determine dosing for later phase clinical trials since patients may prefer to take the drug with a low-fat, low-calorie meal, as daily high-fat meals would be inadvisable. It was therefore determined that undertaking this low-fat food-effect study first would offer the greatest translational value. In this study, a low-fat meal did not affect the rate or extent of mobocertinib absorption, indicating that the drug can be taken without regard to timing of consumption of a low-fat meal. This improves convenience for patients and may enhance treatment adherence.

The 2 oral capsule products of mobocertinib used during the clinical development program were shown to be bioequivalent in the third part of this study. This result suggests that the different synthetic processes and the associated differences in physical properties such as particle size, surface area, and dissolution profiles does not affect oral absorption of mobocertinib in humans. This finding is also consistent with the high solubility and high permeability of mobocertinib.

The results of this study provide additional information to guide mobocertinib dosing as it moves through clinical development, with the goal of providing a novel drug treatment option for patients with NSCLC with *EGFR* exon 20 insertion mutations and *HER2*-activating mutations who currently have no targeted treatment options. Ongoing and planned studies will provide further information on the PK of mobocertinib in patients with renal and hepatic impairment and in special populations (NCT04056455, NCT04056468, NCT03807778).

Conclusions

Single doses of mobocertinib up to 160 mg were tolerated in healthy adult volunteers during clinical pharmacology evaluations. The single-dose PK of mobocertinib was approximately dose-proportional

across a wide dose range (40–160 mg) in healthy volunteers. The geometric mean terminal disposition phase half-life was 20 hours, supporting once-daily dosing of mobocertinib. Administration of mobocertinib with a low-fat meal did not affect plasma PK of mobocertinib, and the 2 capsule products used during clinical development were shown to be bioequivalent. These results guided dosing and supported administration of mobocertinib without regard to low-fat meal intake in subsequent clinical development studies. The results also enabled PK bridging across the 2 different capsule products in the mobocertinib clinical development program.

Acknowledgments

The authors thank the patients, their families, and their caregivers; the investigators and their team members at each study site; and colleagues from Millennium Pharmaceuticals, Inc., Cambridge, Massachusetts, a wholly owned subsidiary of Takeda Pharmaceutical Company Limited. Professional medical writing assistance was provided by Lauren Gallagher, RPh, PhD, and Lela Creutz, PhD, of Peloton Advantage, LLC, an OPEN Health company, Parsippany, New Jersey, and funded by Millennium Pharmaceuticals, Inc.

Conflicts of Interest

S.Z., S.J., C.G., Z.F., J.L., M.B., R.B., and N.G. are employees of Takeda. K.V. is a former employee of Takeda and a current employee of EMD Serono Inc.

Funding

This study was sponsored by Millennium Pharmaceuticals, Inc., Cambridge, Massachusetts, a wholly owned subsidiary of Takeda Pharmaceutical Company Limited.

Data Sharing

The data sets, including the redacted study protocol, redacted statistical analysis plan, and individual participant data supporting the results reported in this article, will be made available within 3 months from initial request, to researchers who provide a methodologically sound proposal. The data will be provided after deidentification, in compliance with applicable privacy laws, data protection, and requirements for consent and anonymization.

References

1. Howlader N, Noone AM, Krapcho M, et al. Cancer of the lung and bronchus (invasive). *SEER Cancer Statistics Review 1975–2016*. 2019. https://seer.cancer.gov/archive/csr/1975_2016/. Accessed June 17, 2020.
2. Roengvoraphoj M, Tsongalis GJ, Dragnev KH, Rigas JR. Epidermal growth factor receptor tyrosine kinase inhibitors as initial therapy for non-small cell lung

- cancer: focus on epidermal growth factor receptor mutation testing and mutation-positive patients. *Cancer Treat Rev.* 2013;39(8):839-850.
3. Yasuda H, Kobayashi S, Costa DB. *EGFR* exon 20 insertion mutations in non-small-cell lung cancer: pre-clinical data and clinical implications. *Lancet Oncol.* 2012;13(1):e23-e31.
 4. Oxnard GR, Lo PC, Nishino M, et al. Natural history and molecular characteristics of lung cancers harboring *EGFR* exon 20 insertions. *J Thorac Oncol.* 2013;8(2):179-184.
 5. Noronha V, Choughule A, Patil VM, et al. Epidermal growth factor receptor exon 20 mutation in lung cancer: types, incidence, clinical features and impact on treatment. *Onco Targets Ther.* 2017;10:2903-2908.
 6. Kobayashi Y, Mitsudomi T. Not all epidermal growth factor receptor mutations in lung cancer are created equal: perspectives for individualized treatment strategy. *Cancer Sci.* 2016;107(9):1179-1186.
 7. Lin YT, Liu YN, Wu SG, Yang JC, Shih JY. Epidermal growth factor receptor tyrosine kinase inhibitor-sensitive exon 19 insertion and exon 20 insertion in patients with advanced non-small-cell lung cancer. *Clin Lung Cancer.* 2017;18(3):324-332.e321.
 8. Kosaka T, Tanizaki J, Paranal RM, et al. Response heterogeneity of *EGFR* and *HER2* exon 20 insertions to covalent *EGFR* and *HER2* inhibitors. *Cancer Res.* 2017;77(10):2712-2721.
 9. Arcila ME, Nafa K, Chaft JE, et al. *EGFR* exon 20 insertion mutations in lung adenocarcinomas: prevalence, molecular heterogeneity, and clinicopathologic characteristics. *Mol Cancer Ther.* 2013;12(2):220-229.
 10. Yang JC, Sequist LV, Geater SL, et al. Clinical activity of afatinib in patients with advanced non-small-cell lung cancer harbouring uncommon *EGFR* mutations: a combined post-hoc analysis of LUX-Lung 2, LUX-Lung 3, and LUX-Lung 6. *Lancet Oncol.* 2015;16(7):830-838.
 11. Wu JY, Wu SG, Yang CH, et al. Lung cancer with epidermal growth factor receptor exon 20 mutations is associated with poor gefitinib treatment response. *Clin Cancer Res.* 2008;14(15):4877-4882.
 12. van Veggel B, Madeira R, Santos JFV, Hashemi SMS, et al. Osimertinib treatment for patients with *EGFR* exon 20 mutation positive non-small cell lung cancer. *Lung Cancer.* 2020;141:9-13.
 13. Arcila ME, Chaft JE, Nafa K, et al. Prevalence, clinicopathologic associations, and molecular spectrum of ERBB2 (*HER2*) tyrosine kinase mutations in lung adenocarcinomas. *Clin Cancer Res.* 2012;18(18):4910-4918.
 14. Shigematsu H, Takahashi T, Nomura M, et al. Somatic mutations of the *HER2* kinase domain in lung adenocarcinomas. *Cancer Res.* 2005;65(5):1642-1646.
 15. Tomizawa K, Suda K, Onozato R, et al. Prognostic and predictive implications of *HER2/ERBB2/neu* gene mutations in lung cancers. *Lung Cancer.* 2011;74(1):139-144.
 16. Vasconcelos PENS, Kobayashi IS, Kobayashi SS, Costa DB. Preclinical characterization of mobocertinib highlights the putative therapeutic window of this novel *EGFR* inhibitor to *EGFR* exon 20 insertion mutations. *JTO Clin Res Rep.* 2021;2(3):100105.
 17. Gonzalez F, Vincent S, Baker TE, et al. Mobocertinib (TAK-788): a targeted inhibitor of *EGFR* exon 20 insertion mutants in non-small cell lung cancer [published online ahead of print February 25, 2021]. *Cancer Discov.*
 18. Janne PA, Neal JW, Camidge DR, et al. Antitumor activity of TAK-788 in NSCLC with *EGFR* exon 20 insertions [abstract]. *J Clin Oncol.* 2019;37(suppl 15):9007.
 19. Hirsh V, Blais N, Burkes R, Verma S, Croitoru K. Management of diarrhea induced by epidermal growth factor receptor tyrosine kinase inhibitors. *Curr Oncol.* 2014;21(6):329-336.
 20. Lacouture ME. Mechanisms of cutaneous toxicities to *EGFR* inhibitors. *Nat Rev Cancer.* 2006;6(10):803-812.
 21. Faucette S, Wagh S, Trivedi A, Venkatakrishnan K, Gupta N. Reverse translation of US Food and Drug Administration reviews of oncology new molecular entities approved in 2011–2017: lessons learned for anticancer drug development. *Clin Transl Sci.* 2018;11(2):123-146.
 22. Ahmed MA, Patel C, Drezner N, Helms W, Tan W, Stypinski D. Pivotal considerations for optimal deployment of healthy volunteers in oncology drug development. *Clin Transl Sci.* 2020;13(1):31-40.
 23. Wang MN, Kuang Y, Gong LY, et al. First-in-human, phase I single-ascending-dose study of the safety, pharmacokinetics, and relative bioavailability of selatinib, a dual *EGFR*-*ErbB2* inhibitor in healthy subjects. *Invest New Drugs.* 2020;38:1826-1835.
 24. Becker A, Martin EC, Mitchell DY, et al. Safety, tolerability, pharmacokinetics, target occupancy, and concentration-QT analysis of the novel BTK inhibitor evobrutinib in healthy volunteers. *Clin Transl Sci.* 2020;13(2):325-336.
 25. Abbas R, Hug BA, Leister C, Gaaloul ME, Chalon S, Sonnichsen D. A phase I ascending single-dose study of the safety, tolerability, and pharmacokinetics of bosutinib (SKI-606) in healthy adult subjects. *Cancer Chemother Pharmacol.* 2012;69(1):221-227.
 26. Sullivan I, Planchard D. Next-generation *EGFR* tyrosine kinase inhibitors for treating *EGFR*-mutant lung cancer beyond first line. *Front Med (Lausanne).* 2017;3:76.
 27. Ding PN, Lord SJ, GebSKI V, et al. Risk of treatment-related toxicities from *EGFR* tyrosine kinase inhibitors: a meta-analysis of clinical trials of gefitinib, erlotinib, and afatinib in advanced *EGFR*-mutated non-small cell lung cancer. *J Thorac Oncol.* 2017;12(4):633-643.
 28. Ruiz-Garcia A, Plotka A, O’Gorman M, Wang DD. Effect of food on the bioavailability of palbociclib. *Cancer Chemother Pharmacol.* 2017;79(3):527-533.
 29. Heath EI, Chiorean EG, Sweeney CJ, et al. A phase I study of the pharmacokinetic and safety profiles of

- oral pazopanib with a high-fat or low-fat meal in patients with advanced solid tumors. *Clin Pharmacol Ther.* 2010;88(6):818-823.
30. Burris HA III, Taylor CW, Jones SF, et al. A phase I and pharmacokinetic study of oral lapatinib administered once or twice daily in patients with solid malignancies. *Clin Cancer Res.* 2009;15(21):6702-6708.
 31. Cho BC, Kim DW, Bearz A, et al. ASCEND-8: a randomized phase I study of ceritinib, 450 mg or 600 mg, taken with a low-fat meal versus 750 mg in fasted state in patients with anaplastic lymphoma kinase (*ALK*)-rearranged metastatic non-small cell lung cancer (NSCLC). *J Thorac Oncol.* 2017;12(9):1357-1367.
 32. Lau YY, Gu W, Lin T, Song D, Yu R, Scott JW. Effects of meal type on the oral bioavailability of the *ALK* inhibitor ceritinib in healthy adult subjects. *J Clin Pharmacol.* 2016;56(5):559-566.
 33. Lentz KA. Current methods for predicting human food effect. *AAPS J.* 2008;10(2):282-288.

Supplemental Information

Additional supplemental information can be found by clicking the Supplements link in the PDF toolbar or the Supplemental Information section at the end of web-based version of this article.